Measurement of Mean Raindrop Shape from Polarimetric Radar Observations

EUGENIO GORGUCCI AND GIANFRANCO SCARCHILLI

CNR Istituto di Fisica dell'Atmosfera, Rome, Italy

V. CHANDRASEKAR AND V. N. BRINGI

Colorado State University, Fort Collins, Colorado

(Manuscript received 6 July 1999, in final form 3 February 2000)

ABSTRACT

Interpretation of polarimetric radar measurements in rainfall such as differential reflectivity and specific differential phase shifts depends on the mean raindrop shape–size relationship. Currently, semiempirical relations between the oblateness and the diameter of the drop are being used. This paper presents an algorithm to obtain the mean shape of the rain drops from polarimetric radar measurements, namely, the reflectivity factor, the differential reflectivity, and the specific differential phase shift. The accuracy of the estimate mean drop shape depends on the measurement accuracies of polarimetric radar observations. Based on asymptotic error analysis and simulations it is shown that the mean raindrop shape can be estimated to an accuracy of 10%. The raindrop shape estimator algorithm developed in this paper is applied to polarimetric radar data collected by the CSU–CHILL radar during the 28 July 1997 Fort Collins, Colorado, flood.

1. Introduction

The mean shape of raindrops plays a critical role in the interpretation of the polarimetric radar measurements. The mean shape raindrop also plays an important role in the development of algorithms to estimate rainfall rate and liquid water content based on reflectivity factor (Z_H), differential reflectivity (Z_{DR}), and specific differential propagation phase (K_{DP}). The equilibrium shape of a raindrop, falling at its terminal fall speed, is determined by the balance between the forces due to surface tension, hydrostatic pressure, and aerodynamic pressure from airflow around the drop. The shapes of raindrops have been studied theoretically by Green (1975) and Beard and Chuang (1987), experimentally in wind tunnels by Pruppacher and Beard (1970), and in natural rainfall using aircraft probes by Chandrasekar et al. (1988) and Bringi et al. (1998). The experimental results of Chandrasekar et al. (1988) and Bringi et al. (1998) were fairly consistent with the model results of Beard and Chuang (1987). All of the above studies as well as polarimetric radar measurements at multiple polarizations show that the shape of raindrops can be approximated by an oblate spheroid, described with an axis ratio (b/a) and equivolumetric spherical diameter D, where a and b are the major and the minor axes of the drop, respectively. A commonly used approximation relating the axis ratio of a raindrop to the diameter is given by (Pruppacher and Beard 1970):

$$b/a = 1.03 - 0.062D. \quad (1)$$

In addition, nonlinear relations are available to model axis ratios of raindrops (Andsager et al. 1999). The experimental results of Bringi et al. (1998) showed that the axis ratios were higher than the model given by (1) for $D < 3$ mm. However, for $D > 4.5$ mm the mean axis ratios were smaller than those given by (1). The above results were obtained after careful and tedious analysis of aircraft-mounted 2D imaging probe data. It would be very useful to obtain an estimate of the mean shape–size relation from polarimetric radar measurements in order to study any variability in the mean shape of the raindrops in different storms as well as different regions of storms.

The objective of this paper is to derive an algorithm to estimate the mean shape of raindrops from polarimetric radar data. The paper is organized as follows. Section 2 defines the mean shape model for raindrops, whereas section 3 describes the effect of raindrop shape on polarimetric radar measurements. The estimator for mean raindrop shape from radar measurements is developed and its accuracy and sensitivity are evaluated in section 4. The estimator developed in this paper is applied to data collected by the CSU–CHILL radar dur-

Corresponding author address: Dr. Eugenio Gorgucci, CNR Istituto di Fisica dell'Atmosfera, Area di Ricerca Roma-Tor Vergata, Via del Fosso del Cavaliere, 100-00133 Rome, Italy.
E-mail: gorgucci@radar.ifa.rm.cnr.it

ing the 28 July 1997 Fort Collins, Colorado, flood and the results are presented in section 5. Section 6 summarizes the important results of the paper.

2. Mean raindrop shape model

Polarimetric radar measurements, wind tunnel measurements, as well as in situ observations using airborne 2D probes indicate that the shape of raindrops can be approximated by oblate spheroids described by semimajor axis a and semiminor axis b. The axis ratio of the raindrop (r) is given by

$$r = \frac{b}{a}. \tag{2a}$$

The equivolumetric spherical diameter is defined by equating the volume of the spheroid to that of a sphere by

$$\frac{\pi}{6}D^3 = \frac{4}{3}\pi a^2 b. \tag{2b}$$

As noted before, the shape versus size relation can be approximated by a straight line given by

$$r = 1.03 - \beta D. \tag{3}$$

In Eq. (3) $r = 1$ when $D \leq 0.03/\beta$, where β is the magnitude of the slope of the shape–size relationship given by

$$\beta = -\frac{dr}{dD}. \tag{4}$$

The approximation given by (1) corresponds to $\beta = 0.062$ mm^{-1}, which is close to the equilibrium shape–size relation, and therefore we denote it by β_e. We note $\beta > \beta_e$ indicates that raindrops are more oblate than equilibrium, whereas $\beta < \beta_e$ indicates raindrops are less oblate (or closer to spherical) than equilibrium.

3. Polarimetric radar measurements: Sensitivity to shape–size relation

The three commonly used polarimetric radar parameters are reflectivity factor at horizontal polarization (Z_H), differential reflectivity (Z_{DR}), and specific differential propagation phase (K_{DP}). Both the cloud model and measurements of raindrop size distribution (RSD) at the surface and aloft show that a gamma distribution model adequately describes many of the natural variations in RSD (Ulbrich 1983):

$$N(D) = n_c f(D) \quad (\text{m}^{-3}\ \text{mm}^{-1}), \tag{5}$$

where $N(D)$ is the number of raindrops per unit volume per unit size interval, n_c is the concentration, and $f(D)$ is the gamma probability density function (pdf), given by

$$f(D) = \frac{\Lambda^{\mu+1}}{\Gamma(\mu + 1)} e^{-\Lambda D} D^{\mu}, \tag{6}$$

where Λ and μ are parameters of the gamma pdf, and Γ indicates gamma function (Abramovitz and Stegun 1970). The parameter N_0 defined by Ulbrich (1983) is related to n_c as

$$n_c = N_0 \frac{\Gamma(\mu + 1)}{\Lambda^{\mu+1}}. \tag{7}$$

The volume-weighted median drop diameter D_0 can be defined as

$$\int_0^{D_0} D^3 N(D)\, dD = \int_{D_0}^{\infty} D^3 N(D)\, dD. \tag{8}$$

The diameter D_0 can be written in terms of the parameters Λ and μ as

$$D_0 = \frac{3.67 + \mu}{\Lambda}. \tag{9}$$

The reflectivity factor $Z_{H,V}$ at horizontal (H) and vertical (V) polarization can be expressed as

$$Z_{H,V} = \frac{\lambda^4}{\pi^5 |k|^2} \int \sigma_{H,V}(D, \beta) N(D)\, dD \quad (\text{mm}^6\ \text{m}^{-3}), \tag{10a}$$

where $\sigma_{H,V}$ denote the radar cross sections at the two linear polarizations; λ is the wavelength; and $k = (\varepsilon_r - 1)/(\varepsilon_r + 2)$, where ε_r is the dielectric constant of water. Similarly, the differential reflectivity (Z_{DR}) and specific differential phase (K_{DP}) can be expressed as

$$Z_{DR} = 10 \log_{10} \frac{\int \sigma_H(D, \beta) N(D)\, dD}{\int \sigma_V(D, \beta) N(D)\, dD} \quad (\text{dB}) \tag{10b}$$

and

$$K_{DP} = \frac{180\lambda}{\pi} \Re \int [f_H(D, \beta) - f_V(D, \beta)] N(D)\, dD \quad (\text{deg km}^{-1}), \tag{10c}$$

where f_H, f_V are the forward scatter amplitudes at H and V polarization states. It can be seen from (10a–c) that for a given RSD, Z_H, Z_{DR}, and K_{DP} can change with shape–size relationship for raindrops.

According to (1), raindrops become more oblate when the size is large. Therefore, the effect of varying shape–size relationship should be more evident in the presence of larger drops. The volume-weighted median drop diameter D_0 is a good indicator of the mean size of drops in the distribution. The effect of varying shape–size relations of raindrops is illustrated by the following analysis. For a given RSD and at S-band frequency, we compute the radar measurements Z_H, Z_{DR}, and K_{DP} for various β in the range of 0.02–0.1 in steps of 0.01. The various shape–size relationships studied here are shown in Fig. 1, where the dash–dotted line represents the equi-

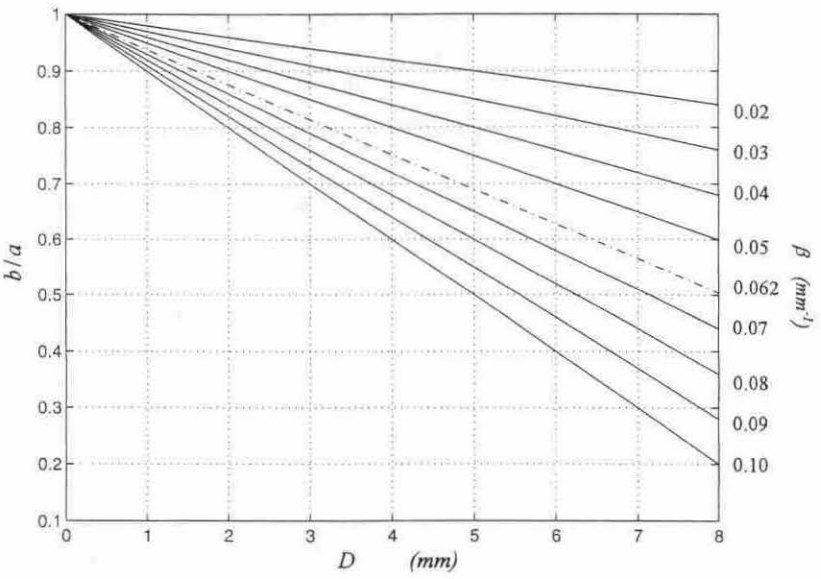

FIG. 1. The raindrop axis ratio (b/a) as a function of the equivolumetric diameter D for different values of the slope β. The dash–dotted line represents the Pruppacher and Beard relation.

librium relation (1). In Fig. 2 the behavior of Z_{DR} (in linear scale) is shown as a function of D_0 for different values of β. It can be noted that Z_{DR} increases as D_0 increases for any value of β (Seliga and Bringi 1976); moreover, for a given D_0, Z_{DR} increases with β. Similar behavior can also be obtained for K_{DP}. As shown in Fig. 2, the sensitivity of Z_{DR} to β is most dependent on D_0. Figure 3a shows the normalized variation of Z_{DR} (in linear scale) with respect to Z_{DR} obtained from the equilibrium relation (1) as a function of β for different values of D_0. For nearly spherical particles ($\beta \cong 0$), the Z_{DR} value should be 0 dB or unity in linear scale. The normalized bias for $\beta \cong 0$ in comparison to β_e is determined by the value of Z_{DR} at $\beta = 0.062$ so that it increases as D_0 increases (see Fig. 2). The range of Z_{DR} difference between nearly spherical drops ($\beta = 0.02$) and equilibrium-shape drops varies between 0.84 and 1.89 dB depending on D_0. Similar arguments can also be made when $\beta > 0$ so that normalized bias of Z_{DR} increases with D_0 as we move farther from $\beta \cong 0$. Figure 3b shows similar analysis for K_{DP}. For nearly spherical particles ($\beta \cong 0$) and $D_0 \leq 1$ mm K_{DP} is approximately zero and then the ratio between K_{DP} with respect to K_{DP} at equilibrium axis ratio is nearly zero and the normalized bias has the maximum negative value equal to -1. By increasing D_0, K_{DP} increases and then the normalized bias decreases. Similar results can be obtained for $\beta > 0$ so that the normalized bias decreases by increasing D_0. The reflectivity factor is fairly insensitive to raindrop shape–size relationships for $\beta < \beta_e$ as shown in Fig. 3b, whereas for $\beta > \beta_e$ the change in Z_H with β is within 10%.

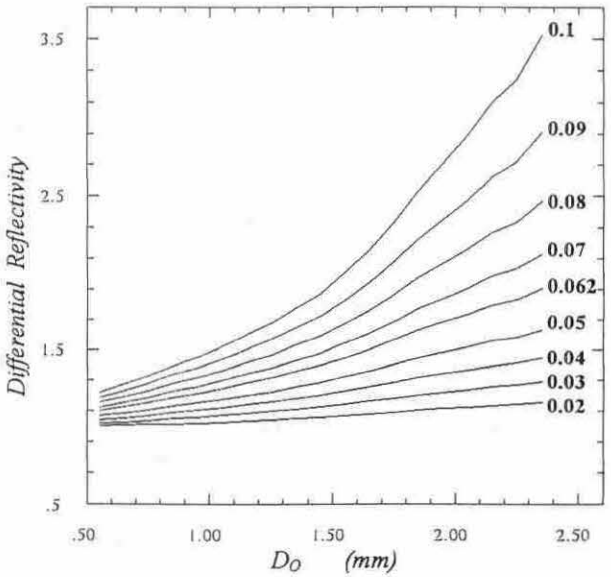

FIG. 2. Averaged value of differential reflectivity (in linear scale), as a function of median drop diameter (D_0) for different values of β, for various RSD.

4. Algorithm to estimate raindrop shape–size relation

The result of section 3 indicates that the observations of Z_{DR} and K_{DP} are sufficiently sensitive to β, so that it can be turned around into measurement. The estimator of β is developed using the following procedure. First, large number of Gamma RSD is simulated over a wide range of the parameters N_0, D_0, and μ, as suggested by

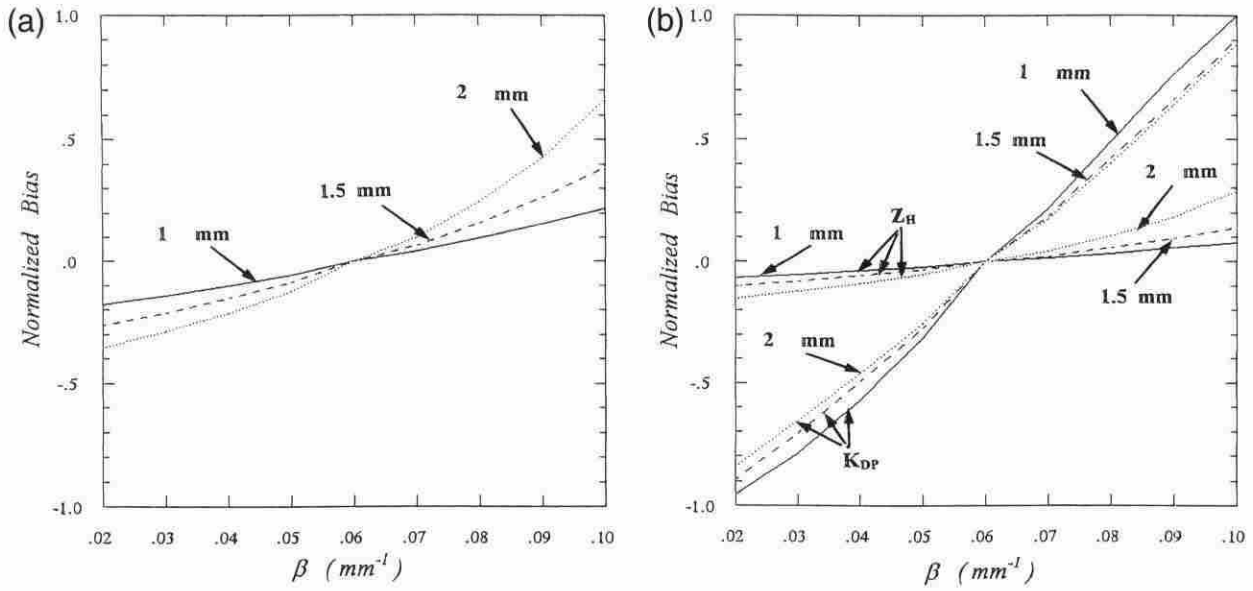

FIG. 3. Normalized bias (a) on the differential reflectivity (Z_{DR}), in linear scale, with respect to Z_{DR}, and (b) on the reflectivity factor (Z_H) and specific differential phase (K_{DP}) with respect to Z_H and K_{DP}, obtained from Pruppacher and Beard relation as a function of the slope β, for the values of the median drop diameter D_0 corresponding to 1 mm (solid line), 1.5 mm (dashed line), and 2 mm (dotted line).

Ulbrich (1983), chosen randomly in the following intervals:

$$-1 < \mu < 4 \tag{11a}$$

$$10^{3.2+0.216\mu} < N_0 < 10^{4.5+0.55\mu} \quad (\text{m}^{-3}\ \text{mm}^{-1-\mu}) \tag{11b}$$

$$0.5 < D_0 < 2.5 \quad (\text{mm}). \tag{11c}$$

In addition, for each RSD, Z_H, Z_{DR}, and K_{DP} are computed for various values of β ranging between 0.02 and 0.1. The above computations are done at S-band frequency. Subsequently, nonlinear regression analysis is performed to evaluate various functional forms to estimate β. The above analysis yields the estimator for β at the S band given (Gorgucci et al. 1999a)

$$\beta = 2.37 Z_H^{-0.377} K_{DP}^{0.396} \times 10^{0.093 Z_{DR}}. \tag{12}$$

A scattergram between β and the true value of β is shown in Fig. 4; it can be noted that (12) estimates β fairly well. The data used in Fig. 4 have a correlation of 0.996 with a normalized standard error (the root-mean-square error normalized with the mean) of 3.6%.

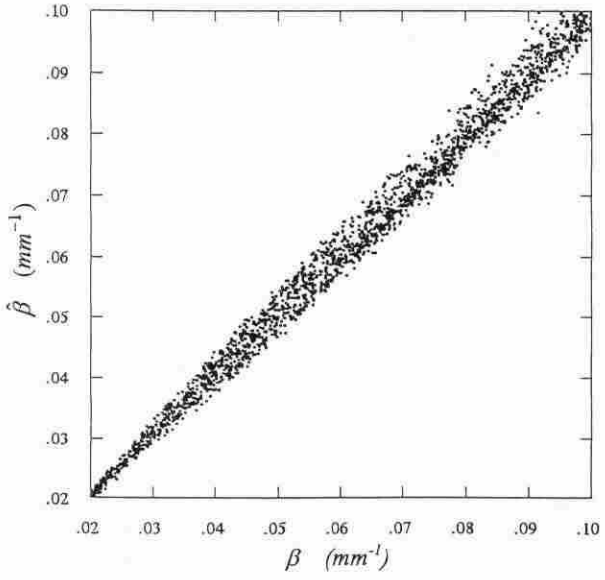

FIG. 4. Scatter diagram between the slope β and the estimate β computed by (12) in absence of measurement errors on radar observables.

a. *Shape–size relation estimate in the presence of measurement errors*

The estimate given by (12) uses Z_H, Z_{DR}, and K_{DP}. These three measurements have completely different error structure. The Z_H is based on absolute power measurement and has a typical accuracy of 1 dB. The Z_{DR} is a relative power measurement and is the differential power estimate between Z_H and Z_V. It can be estimated to an accuracy of 0.2 dB. The K_{DP} is the slope of the range profile of the differential propagation phase Φ_{DP}, which can be estimated to an accuracy of a few degrees. The subsequent estimate of K_{DP} depends on the procedure used such as a simple finite-difference scheme or a least squares fit. Using a least squares estimate of the Φ_{DP} profile, the standard deviation of K_{DP} can be expressed as (Gorgucci et al. 1999b)

$$\sigma(K_{DP}) = \sqrt{3}\frac{\sigma(\Phi_{DP})}{N\Delta r}\sqrt{\frac{N}{(N-1)(N+1)}}, \tag{13}$$

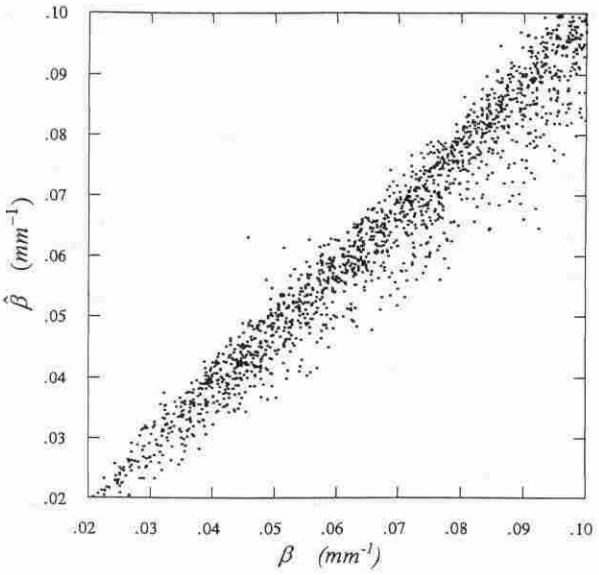

FIG. 5. Scatter diagram between the slope β and the estimate β computed by (12) in presence of measurement errors on radar observables.

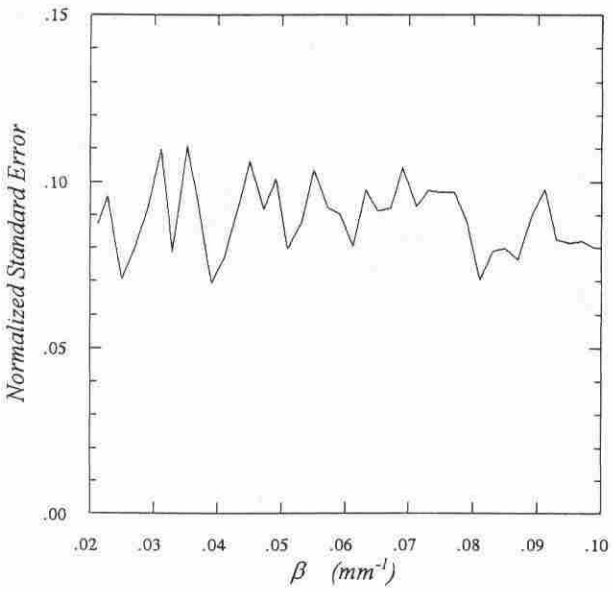

FIG. 6. Normalized standard error of the estimate β computed by (12) as a function of the slope β.

where Δr is the range resolution of the Φ_{DP} estimate and N is the number of range samples within the path. For large N we can see that $\sigma(K_{DP})$ decreases as $N^{-3/2}$. For a typical 150-m range spacing, and with 2.5° accuracy of Φ_{DP}, the K_{DP} can be estimated, over a path of 3 km, with a standard error of 0.32° km^{-1}. Thus, the three measurements Z_H, Z_{DR}, and K_{DP} have completely different error structure. In addition, the measurement errors of Z_H, Z_{DR}, and K_{DP} are nearly independent. In the following we use simulations to quantify the error structure of the estimate of β. The simulation is done as follows. Various rainfall values are simulated varying the parameters of the gamma RSD over a wide range of values, as suggested by Ulbrich (1983). For each RSD the corresponding Z_H, Z_{DR}, and K_{DP} are evaluated using (10a–c). The random measurement errors are simulated using the procedure described in Chandrasekar et al. (1986). The principal parameters of our simulation are as follows: 1) wavelength $\lambda = 11$ cm; 2) sampling time PRT = 1 ms; 3) number of samples pairs $M = 64$; 4) Doppler velocity spectrum width $\sigma_v = 2$ m s^{-1}; 5) cross correlation between H and V signals $\rho_{HV} = 0.99$; 6) range sample spacing over the path where K_{DP} is estimated is 150 m; and 7) K_{DP} is estimated over a path of 50 range samples, as a least squares fit on Φ_{DP} measurements. Figure 5 shows the scatter diagram of β given by (12) versus β in the presence of measurement errors, using K_{DP} values greater than 0.4° km^{-1}. The scatter diagram of the data in Fig. 5 gives a correlation coefficient of 0.97 and a normalized standard error of 9%. Finally, Fig. 6 shows the normalized standard error of β as a function of β, where normalized standard error is defined as the root-mean-square error normalized with respect to the mean. The results of Fig. 6 show that the slope of the shape–size relation β can be estimated to an accuracy of about 9% in the presence of measurement errors in Z_H, Z_{DR}, and K_{DP}. The appendix shows variance computations of β only due to measurement errors.

b. *Sensitivity of mean shape estimation to bias in Z_H and Z_{DR}*

Bias errors in Z_H and Z_{DR} can affect the estimate of β. Bias errors in the measurements of Z_H and Z_{DR} will remain even if extensive averaging is performed. The term Z_{DR} is a differential power measurement and its bias can be estimated and removed easily (Gorgucci et al. 1999b). However, Z_H is based on absolute power measurement and it is difficult to get the absolute calibration. Typically this can be known to an accuracy of 1 dB. Thus K_{DP} is based on phase measurement and is immune to calibration biases in fairly uniform rain medium. The bias in β due to bias errors in Z_H and Z_{DR} can be defined as

$$\text{bias}(\hat{\beta}) = \frac{E[\hat{\beta}(\text{with bias in } Z_H, Z_{DR})]}{E[\hat{\beta}(\text{with no bias in } Z_H, Z_{DR})]}. \quad (14)$$

Figure 7 shows contours of bias in the estimate of β as a function of bias in Z_H and Z_{DR}. The contours line marked 1 indicates no bias, and lines marked different from 1 indicate overestimation (>1) and underestimation (<1). Typically in a well-maintained system, bias error in Z_{DR} is less than 0.2 dB and bias in Z_H is less than 1 dB. Therefore, from Fig. 7 it can be seen that β can be estimated within 10% accuracy under those biases of Z_H and Z_{DR}.

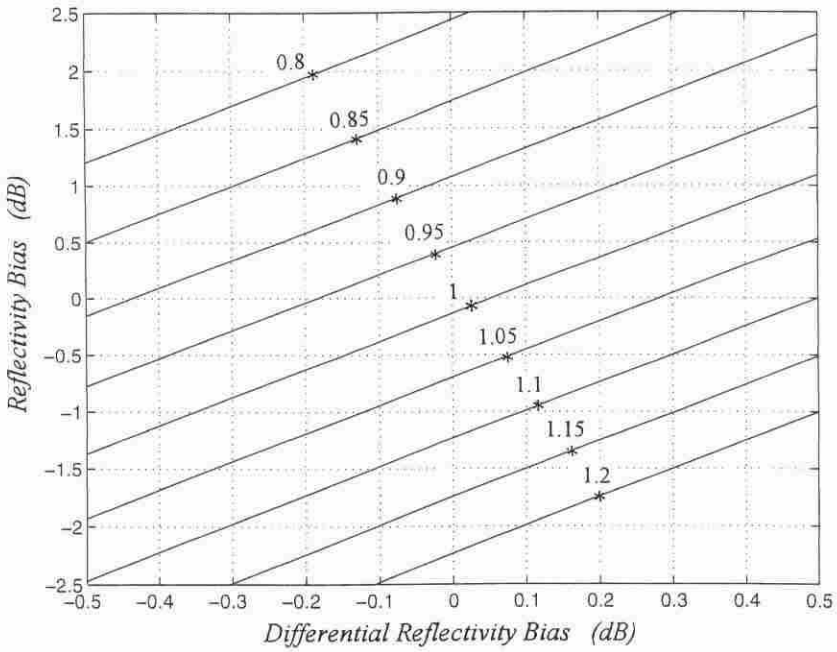

FIG. 7. Contours of bias in the estimate of the slope β as a function of biases in the reflectivity (Z_H) and differential reflectivity (Z_{DR}). The contour line marked 1 indicate no bias, whereas lines marked >1 indicate overestimation and <1 underestimation, respectively.

5. Data analysis

On the evening of 28 July 1997, the city of Fort Collins was hit by a flash flood that caused fatalities and extensively property damage. Mesoscale analysis of this flood is described in Petersen et al. (1999). CSU–CHILL radar recorded continuous data over the event, collecting multiparametric measurements over 5 h. The radar recorded measurements of Z_H, Z_{DR}, and K_{DP}. The characteristics of the CSU–CHILL radar that are relevant for this paper are listed in Table 1. The application of algorithm (12) is fairly straightforward, but numerous details are important. A linear least squares fit was done on the Φ_{DP} observations to obtain one K_{DP} estimate for a 3-km path, whereas Z_H and Z_{DR} are computed as the mean value of Z_H and Z_{DR} measurements on the same path. These values of Z_H, Z_{DR}, and K_{DP} were used in (12) to estimate β. Only data from regions with $K_{DP} > 0.4°$ km^{-1} were used to ensure good accuracy in the estimate of β. A histogram of the various observed values of β, for reflectivity in the range of 40 to 45 dBZ, is shown in Fig. 8a, where the mean and standard deviation of data are 0.061 and 0.01 respectively. The standard deviation of data in Fig. 8a is fairly close to measurement standard deviation, as shown in the appendix. Therefore, most of the spread in β is due to measurement error. In addition, it can be seen that the mean slope of shape–size relation shown in Fig. 8a is close to the theoretical predictions as well as to experimental observation reported in the literature so far (Beard and Chuang 1987; Chandrasekar et al. 1988; Bringi et al. 1998). Figure 8b shows similar results for data corresponding to 45 dBZ $< Z_H <$ 50 dBZ. The mean β and standard deviation of the data shown in Fig. 8b are 0.057 and 0.008, respectively. Once again it can be seen that most of the standard deviation is due to measurement error, and the mean β of 0.057 indicates that the drops are less oblate than β_e perhaps due to drop oscillations (Beard et al. 1983). Similar stratification was continued for reflectivity ranging between 50 and 53 dBZ and for $Z_H >$ 53 dBZ. Figure 8c shows

TABLE 1. System characteristics of the CSU–CHILL radar.

	Antenna
Antenna type	Center-fed paraboloid
Antenna size	8.5 m
3-dB beamwidth	1.1°
Gain	45 dB
Sidelobe level	≤−27 dB
Polarization radiated	Linear, horizontal, or vertical
Feed	Dual-mode conical horn
	Transmitter
Wavelength	10.7 cm
Peak power	700–1000 kW
Pulse width	Steps of 0.1 μs up to 1 μs
PRT	800–2500 μs
Type	Kystron, modernized FPA-18
Max unambiguous range	375 km
Max unambiguous velocity	±34.3 m s^{-1}
	Receiver
Noise figure	3.4 dB
Transfer function	Linear
Dynamic range	96 dB, 0–60 dB IAGC in 12-dB steps
Min detectable signal	−115 dBm

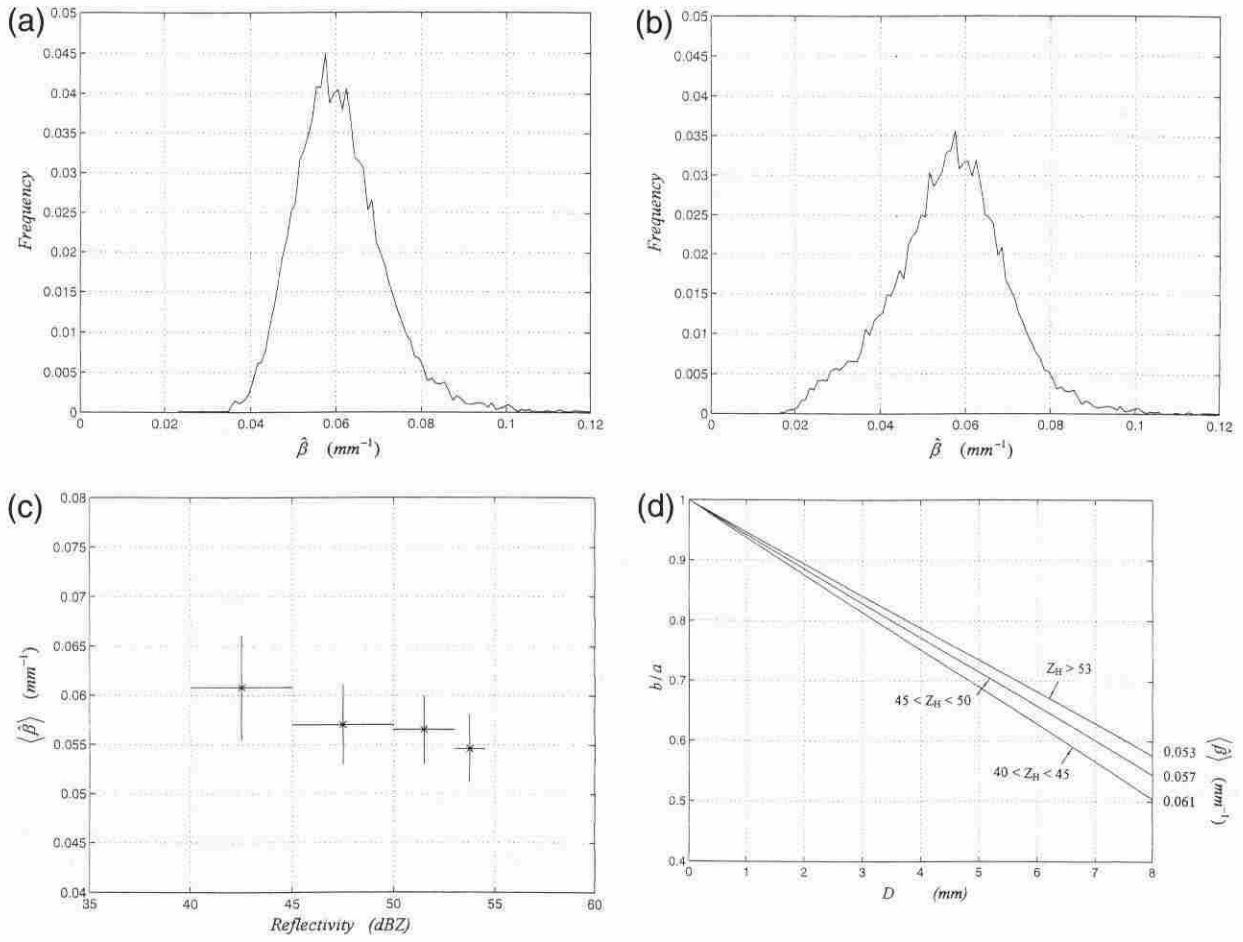

FIG. 8. (a) Histogram of observed values of the estimate β, computed by (12), for reflectivity factor ranging between 40 and 45 dBZ. The data referring to a flash flood that occurred over Fort Collins were collected by the Doppler and polarimetric CSU–CHILL radar. (b) Histogram of observed values of the estimate β, computed by (12), for reflectivity factor ranging between 45 and 50 dBZ. The data referring to a flash flood that occurred over Fort Collins were collected by the Doppler and polarimetric CSU–CHILL radar. (c) The mean value of the estimate β, signed by star, and the corresponding standard deviation for reflectivity intervals 40–45, 45–50, and 50–53 dBZ and for reflectivity greater than 53 dBZ. The data referring to a flash flood that occurred over Fort Collins were collected by the Doppler and polarimetric CSU–CHILL radar. (d) Observed shape–size relation for the values of mean β computed for the reflectivity intervals corresponding to $40 < Z_H < 45$ dBZ, $45 < Z_H < 50$, and for $Z_H > 53$ dBZ. The data referring to a flash flood that occurred over Fort Collins were collected by the Doppler and polarimetric CSU–CHILL radar.

the estimate of mean β and its standard deviation as a function of reflectivity. The standard deviation was computed for each case and was found to range between 18% and 13% around the mean. Figure 8d shows the observed mean shape–size relations, stratified with reflectivity. It can be seen from Figs. 8c and 8d that the axis ratios become progressively slightly less oblate in comparison to equilibrium axis ratios probably due to raindrop oscillations.

6. Summary and conclusions

The mean shape–size relation of raindrops plays an important role in the interpretation of polarimetric radar measurements. The polarimetric radar algorithms available in the literature have been developed for equilibrium axis ratios. A simple model was developed to describe the shape–size relation of raindrops in terms of the slope (β) of the linear approximation to the shape–size function. Subsequently, theoretical analysis was utilized to quantify the variability in Z_H, Z_{DR}, and K_{DP} due to changes in β. The sensitivity of Z_H, Z_{DR}, and K_{DP} to deviation from equilibrium shape–size relation β_e was studied. It was found that both Z_{DR} and K_{DP} were fairly sensitive to changes in β, whereas Z_H was insensitive as expected. There was enough sensitivity to β in Z_{DR} and K_{DP} that it could be turned around to a measurement. An algorithm to estimate the slope of the shape–size relation was derived. The algorithm can be used to estimate β from measurements of Z_H, Z_{DR}, and K_{DP}. Error analysis of the algorithm demonstrated that the algorithm estimates β on the average to an accuracy of 9%, when K_{DP} is estimated over a path of 50 range bins with a range spacing of 150 m. Polarimetric radar data col-

lected by the CSU–CHILL radar was used to evaluate the algorithm developed in this paper. The estimation of β from radar data yielded values very close to the equilibrium shape–size relation of raindrops. When the data were stratified with reflectivity, the results indicated that the drops became less oblate as reflectivity increases, an indication of possible raindrop oscillation.

Acknowledgments. This project was supported by the National Science Foundation (ATM-9413453), by the National Group for Defense from Hydrological Hazards (CNR, Italy), by Progetto Strategico Mesoscale Alpine Program (CNR, Italy), by the Italian Space Agency (ASI), and by the NASA TRMM program. The CSU–CHILL is supported by the National Science Foundation (ATM-9500108). The gauge data were collected and archived by the Colorado Climate Center, and the radar data were collected by Bob Bowie of the CSU–CHILL facility. The authors are grateful to A. Mura and P. Iacovelli for assistance rendered during the preparation of the manuscript.

APPENDIX

Variance in the Estimate of Mean Shape–Size Relation (β)

The estimate for β is given by

$$\beta = cZ_H^{a_1}K_{DP}^{a_2} \times 10^{-a_3 Z_{DR}}, \quad \text{(A1)}$$

where a_1, a_2, a_3, and c are the coefficients given by (12). The variance of β normalized to the mean value can be expressed from perturbation analysis as

$$\frac{\mathrm{var}(\hat{\beta})}{\hat{\beta}^2} = a_1^2 \frac{\mathrm{var}(Z_H)}{Z_H^2} + a_2^2 \frac{\mathrm{var}(K_{DP})}{K_{DP}^2} + (a_3 \ln 10)^2 \mathrm{var}(Z_{DR}). \quad \text{(A2)}$$

Note that Z_H can be measured to an accuracy of better than 1 dB, Z_{DR} can be measured to an accuracy of 0.2 dB, and standard deviation in the estimate of K_{DP} is given by (12). Assuming 20 range bins with range spacing of 0.15 km and for a mean value of K_{DP} of 0.86° km^{-1}, the normalized standard error (standard deviation normalized with respect to the mean) of β is 15%.

REFERENCES

Abramovitz, M., and A. Stegun, 1970: *Handbook of Mathematical Functions.* Dover, 1043 pp.

Andsager, K., K. V. Beard, and N. F. Laird, 1999: Laboratory measurements of axis ratios for large raindrops. *J. Atmos. Sci.*, **56,** 2673–2683.

Beard, K. V., and C. Chuang, 1987: A new model for the equilibrium shape of raindrops. *J. Atmos. Sci.*, **44,** 1509–1524.

——, D. B. Johnson, and A. R. Jameson, 1983: Collisional forcing of raindrop oscillations. *J. Atmos. Sci.*, **40,** 455–462.

Bringi, V. N., V. Chandrasekar, and R. Xiao, 1998: Raindrop axis ratio and size distributions in Florida rainshafts: An assessment of multiparameter radar algorithms. *IEEE Trans. Geosci. Remote Sens.*, **36,** 703–715.

Chandrasekar, V., V. N. Bringi, and P. J. Brockwell, 1986: Statistical properties of dual polarized radar signals. Preprints, *23rd Conf. on Radar Meteorology,* Snowmass, CO, Amer. Meteor. Soc., 154–157.

——, W. A. Cooper, and V. N. Bringi, 1988: Axis ratios and oscillation of raindrops. *J. Atmos. Sci.*, **45,** 1325–1333.

Gorgucci, E., G. Scarchilli, and V. Chandrasekar, 1999a: Estimation of mean raindrop shape from polarimetric radar measurements. Preprints, *29th Int. Conf. on Radar Meteorology,* Montreal, PQ, Canada, Amer. Meteor. Soc., 168–171.

——, ——, and ——, 1999b: A procedure to calibrate multiparameter weather radar using properties of the rain medium. *IEEE Trans. Geosci. Remote Sens.*, **37,** 269–276.

Green, A. W., 1975: An approximation for the shapes of large raindrops. *J. Appl. Meteor.*, **14,** 1578–1583.

Petersen, A. P., and Coauthors, 1999: Mesoscale and radar observations of the Fort Collins flash flood of 28 July 1997. *Bull. Amer. Meteor. Soc.*, **80,** 191–216.

Pruppacher, H. R., and K. V. Beard, 1970: A wind tunnel investigation of the internal circulation and shape of water drops falling at terminal velocity in air. *Quart. J. Roy. Meteor. Soc.*, **96,** 247–256.

Seliga, T. A., and V. N. Bringi, 1976: Potential use of the radar reflectivity at orthogonal polarizations for measuring precipitation. *J. Appl. Meteor.*, **15,** 69–76.

Ulbrich, C. W., 1983: Natural variations in the analytical form of raindrop size distributions. *J. Climate Appl. Meteor.*, **22,** 1764–1775.